UCRL- 86326
PREPRINT

CONF-811140--1

UTILIZING SUBCOOLED, SUPERFLUID He-II IN THE DESIGN OF A 17-TESLA TANDEM-MIRROR EXPERIMENT

R. W. Heard and D. N. Cornish
R. W. Baldi and W. D. Taylor (General Dynamics)

This paper was prepared for submittal to
Workshop on the Stability of Superconductors in He-I and He-II
Saclay, France
November 16-19, 1981

November 11, 1981

UTILIZING SUBCOOLED, SUPERFLUID He-II IN THE DESIGN OF A 12-TESLA TANDEM MIRROR EXPERIMENT

R. W. HOARD and D. N. CORNISH
University of California, Lawrence Livermore National Laboratory
Livermore, CA 94550 (U.S.A.)
R. W. BALDI and W. D. TAYLOR
General Dynamics, Division of Convair, San Diego, CA 92138 (U.S.A.)

SUMMARY

A design study of 12-T yin-yang coils for a conceptual Tandem Mirror Next Step (TMNS) facility has been recently performed by Lawrence Livermore National Laboratory in conjunction with the Convair Division of General Dynamics. The large magnets have major and minor radii of 3.7 and 1.5 m, 0.70 x 3.75 m^2 cross section, 46.3 MA turns, and an overall current density of 1765 A/cm^2, obtained by the use of Nb_3Sn and Nb-Ti superconductors. Each coil is composed of several subcoils separated by internal strengthening substructure to react the enormous electromagnetic forces. The size of the yin-yang coils, and hence the current density, was reduced by utilizing subcooled, superfluid He-II at 1.8 K for the coolant. This paper reviews the design study, with emphasis on He-II heat transport and conductor stability. Methods are also presented which allow the extension of Gorter-Mellink-channel calculations to encompass multiple, interconnecting coolant channels.

1. INTRODUCTION

Development work is continuing on the magnetic mirror fusion program at Lawrence Livermore National Laboratory (LLNL). The main emphasis is on the design of experimental machines that will ultimately produce a full-scale, commercial power reactor. Current efforts have been concentrated on the Mirror Fusion Test Facility (MFTF), which has yin-yang end-plug magnets operating at 7.68 T, utilizing Nb-Ti conductor, with 4.2 K liquid-helium (LHe) cooling. Following the successful construction and operation of MFTF, the next proposed experiment is the Tandem Mirror Next Step (TMNS) facility. This machine has superconducting yin-yang coils requiring higher fields of 12 T with both Nb-Ti and Nb_3Sn conductor. The coil parameters include: a major radius of 3.7 m, minor radius of 1.5 m, coil cross section of 0.70 x 3.75 m^2, sweep angle of 65°, 46.3 MA turns, and an overall current density of 1765 A/cm^2. Figure 1 shows the total magnet configuration of the TMNS facility, while Fig. 2 displays an enlarged, computer-generated view of a nested yin-yang magnet pair. Since the magnetic forces scale as B^2, more massive internal strengthening structure must be used (to minimize strains on the Nb_3Sn conductor), which in turn lowers the overall current density and allowable space for coolant channels. Therefore, subcooled superfluid He-II has been designated to provide heat-transfer fluxes of approximately 0.8 W/cm^2.

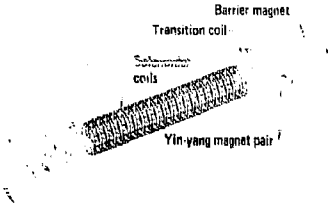

Fig. 1 - TMNS magnet configuration

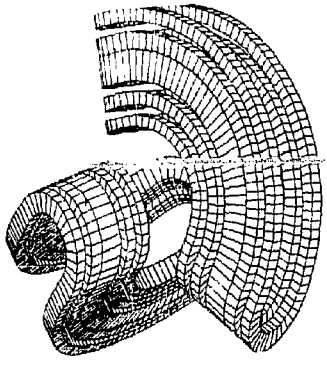

Fig. 2 - Nested yin-yang coils for TMNS: spaces between subcoils are for substructure

This paper, in conjunction with Refs. /1,2/, summarizes the results of the TMNS 12-T yin-yang magnet design study, with particular concentration on the subjects of He-II heat transport, coolant-channel geometry, and conductor stability. The primary interest is in incorporating into the magnet design flow channels for the He-II coolant that permit steady-state stabilization of a normal zone on a single turn of superconducting, composite conductor. The problem is best solved by reviewing the heat generation in the conductor in the event of a possible superconducting-to-normal transition and understanding the heat-transfer properties of the He-II coolant.

2. HEAT GENERATION IN THE CONDUCTOR

Figure 3 shows a plot of the heat generated in the conductor as a function of its temperature. The resultant heat production (W/cm^2) can be summarized as /3/

$$
\begin{aligned}
G &= 0, && T_b \leqslant T < T_{cs}, \\
G &= I\left[I - I_c\left(\frac{T_c - T}{T_c - T_b}\right)\right]\frac{\rho}{P_s A_c}, && T_{cs} \leqslant T < T_c, \\
G &= \frac{I^2 \rho}{P_s A_c}, && T_c \leqslant T,
\end{aligned}
\tag{1}
$$

where I_c and T_c are the critical values obtained at 1.8 K and at applied field H_a, T_b is the starting bulk temperature of the coolant bath, ρ and A_c are the resistivity and area of the nonsuperconducting composite component (usually the copper matrix), P_s is the conductor perimeter, and T_{cs} is the temperature at which current sharing begins between the superconducting filaments, composite matrix, and copper stabilizer. T_{cs} is given by

$$
T_{cs} = T_b + \left(1 - \frac{I}{I_c}\right)\left(T_c - T_b\right). \tag{2}
$$

3. STEADY-STATE HEAT TRANSFER TO He-II IN GORTER-MELLINK CHANNELS

Figure 3 also shows the heat-transfer curve of an open coolant channel immerged in superfluid He-II. The low-flux region is determined by the Kapitza conductance, a little understood phenomenon in which heat is conducted by an apparent radiant transport of phonons between the conductor surface and the He-II. For copper to He-II, it takes the form of

$$
q_k = \frac{Q}{P_s} = 0.02\left(T^4 - T_b^4\right)\frac{W}{cm^2}, \qquad T_b < T < T_m. \tag{3}
$$

Beyond the Kapitza region, the heat transfer becomes constant (with respect to temperature), taking on a value which appears to be a function of channel length only /4/

outward flow of He-I fluid (away from the heat source) with an inward motion of the He-II fluid component (towards the heat source). The He-II fluid components then undergo transitions to normal He-I fluid at the conductor surface. At the temperature T^*, all the LHe in thermal contact with the conductor has been converted to normal He-I and film boiling commences.

These heat transfer and generation regions are graphically depicted in Fig. 3 with the corresponding transitional temperatures. T_m is defined when the Kapitza heat transfer equals the flat critical value of eq. (4b):

$$T_m = \left(\frac{\bar{q}_c}{0.02} + T_b^4 \right)^{1/4} . \tag{5}$$

Assuming that in the film boiling region $\bar{q}$ is linear with temperature, T^* is the temperature at which $\bar{q}_c$ intercepts the film boiling line:

$$T^* = T_b + \frac{q_c}{h} , \tag{6}$$

since

$$q_f = h(T - T_b) \text{ with } h \gtrsim 0.1 \text{ W/cm}^2 \text{ K}. \tag{7}$$

T_f is defined by the interception of the I^2R heating curve with the film boiling region:

$$T_f = T_b + \frac{I^2 \rho}{A_c P_s h} . \tag{8}$$

4. STEADY-STATE HEAT TRANSFER IN MULTIPLE, INTERCONNECTING COOLANT CHANNELS

Equation (4) has been shown to be valid for single Gorter-Mellink cooling channels. However, most practical fusion magnets have interturn and interlayer insulation that create multiple, interconnecting coolant channels. Figure 4 shows

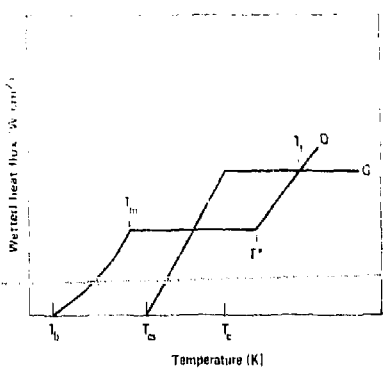

Fig. 3 - Generated (G) and heat-transfer (Q) curves for a conductor in He-II

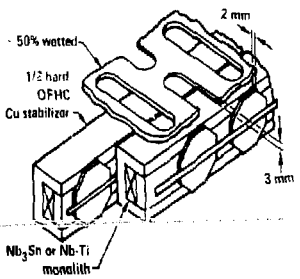

Fig. 4 - TMNS conductor and insulation arrangement

the TMNS conductor, the interlayer insulation, and the arrangement of the octagon-button interturn insulation. A schematic cross section of the conductor pack with associated cooling channels is depicted by Fig. 5. A possible way to extrapolate the results of Section 3 to encompass multiple, branching cooling-channel network is by following the diffusion of horizontal and vertical heat fluxes emanating from a normal turn "X." Eight coolant channels leave the conductor surface; these are increased to 16 after passing zone 1, 24 after zone 2, 32 after zone 3, ... In general, the evolution of the fluxes can be represented as

$$q_{h,v} = q_{0h,v}/N , \tag{9}$$

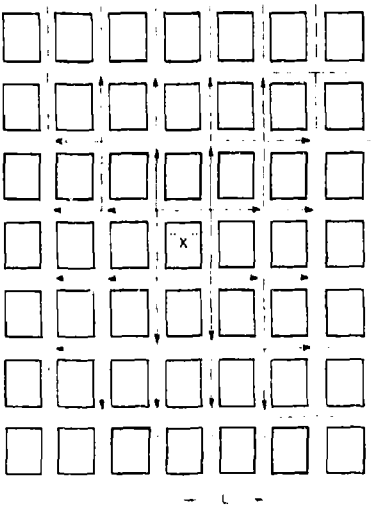

Fig. 5 - Cooling channels accessible to normal turn "X" via neighboring conductor zones

where $q_{h,v}$ are the horizontal and vertical heat fluxes after spreading through zone N and $q_{0h,v}$ are their starting values at the conductor surface. The dissipation and spreading of a single, horizontal-channel heat flux is depicted in Fig. 6 as it leaves the normal conductor X. The steady-state, heat-transport equation for He-II is given by

$$\nabla T = f(T)q^3 , \tag{10}$$

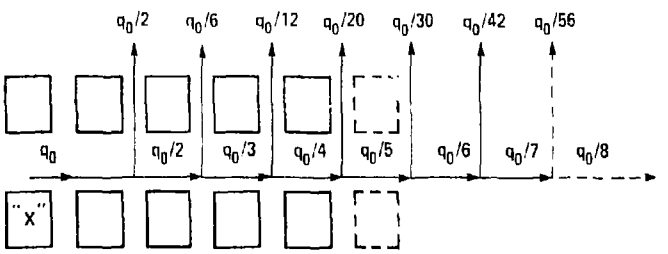

Fig. 6 - Decrease of heat flux as it migrates across one horizontal channel

in which f is a temperature-dependent resistance function. Equation (10) can be integrated between the bath temperature of 1.8 K and the temperature adjacent to the conductor T_λ over the total channel length, while including the decline of the horizontal heat flux with channel length

$$\int_{1.8}^{T} \frac{dT}{f(T)} = \int_{0}^{L_1} q_0^3 dx + \int_{L_1}^{L_2} \frac{q_0^3}{8}\, dx + \int_{L_2}^{L_3} \frac{q_0^3}{27}\, dx + \ldots + \int_{L_{n-1}}^{L_n} \frac{q_0^3}{n^3}\, dx. \tag{11}$$

Solving for q_0, the maximum permissible steady-state heat flux that can be conducted through the horizontal channel, yields

$$q_0 = \frac{7.4}{\Delta L^{1/3} \left(\sum_{n=1} 1/n^3 \right)^{1/3}} , \tag{12}$$

in which ΔL is the channel pitch length between conductors, and the summation of $1/n^3$ terms is the Riemann zeta function $\zeta(3)$, which rapidly converges to 1.20205. Equation (12) then becomes

$$q_0 = \frac{7.4}{(1.063)\,\Delta L^{1/3}} . \tag{13}$$

The significance of eq. (13) is that the multiple, interconnecting cooling channels of a rectangular array of conductor pack can be modeled as a simple Gorter-Mellink channel, with a length equal to the conductor pitch distance. With the channel length so defined, using eq. (4) instead of (13) introduces only a 6% error in calculating the maximum heat flux and, therefore, a 3% error in the corresponding full-recovery current.

This section concerns the design of He-II coolant channels for the 12-T Nb_3Sn yin-yang magnets for TMNS. Figure 4 shows the conductor, interlayer, and interturn G-10 insulation. The problem entails designing adequate He-II cooling channels within the G-10 insulation spaces. The various calculated steps are summarized and tabulated below.

Cross-sectional area of the total conductor copper: $A_{Cu} = 4.897\ cm^2$
Effective copper resistivity: $\rho = 6.802 \times 10^{-8}\ \Omega \cdot cm$
Normal conductor generated power per unit length: $P/\ell = Q = I^2\rho/A_{Cu} = 3.380\ W/cm$
Volume of He-II surrounding each conductor per unit length: $V_0 = 1.058\ cm^3/cm$
Conductor wetted surface area per unit length: $A_{ws} = 4.119\ cm^2/cm$
Conductor wetted heat flux: $q_c = P/A_{ws}\ell = 0.821\ W/cm^2$.

The normal conductor temperature due to Kapitza resistance is $T_k = 2.65$ K, which is less than the current-sharing temperatures, 4.2 and 2.83 K for the Nb_3Sn and Nb-Ti conductors.

Figure 5 shows a schematic cross section of a bundle of conductors and their associated He-II cooling channels. Notice that there are actually eight cooling channels that surround each conductor length (four horizontal and four vertical). In general, the heat flux will not flow equally through each, but will predominately travel through the channel having the smallest resistance for heat transport to an additional volume of He-II. This concept defines a He-II coolant conductance for the horizontal and vertical channels. From eq. (4),

$$\frac{Q}{A} = F\,\Delta T^{1/3} = F\,\frac{\Delta T^{2/3}}{\Delta L^{1/3}}\,\Delta T = C\,\Delta T ,$$

where C is the channel conductance. The heat flux

$$q_h = \frac{Q}{4}\left(\frac{C_h}{C_h + C_v}\right)$$

flows into each horizontal channel, where

$$C_h \approx A_h/L_h^{1/3} \quad \text{and} \quad C_v \approx A_v/L_v^{1/3} .$$

Thus,

$$q_h = \frac{Q}{4}\left[\frac{1}{1 + \frac{A_v}{A_h}\left(\frac{L_h}{L_v}\right)^{1/3}}\right]. \tag{14}$$

Similarly, the heat flux

$$q_v = \frac{Q}{4}\left[\frac{1}{1 + \frac{A_h}{A_v}\left(\frac{L_v}{L_h}\right)^{1/3}}\right] \tag{15}$$

flows into each vertical channel. In eqs. (14) and (15), A_v, A_h, L_v, and L_h are the vertical and horizontal coolant channel cross-sectional areas and channel lengths.

In this study, L is defined as the maximum length that a given heat flux travels before it is split or subdivided by flowing into a connecting cooling channel. From Fig. 5, this is shown by the arrows to be the distance from the middle of the normal conductor to just beyond the first zone of nearest neighboring conductors. For the TMNS conductor design, these distances are

$$L_v = 4.586 \text{ cm and } L_h = 3.198 \text{ cm; also } A_v = 0.222 \text{ cm}^2 \text{ and } A_h = 0.577 \text{ cm}^2. \quad (16)$$

Utilizing eqs. (14-16) and a power production of 3.380 W/cm length of normal conductor turn, we obtain for each horizontal and vertical channel in TMNS

$$q_h = 3.97 \text{ W/cm}^2, \text{ and } q_v = 3.52 \text{ W/cm}^2 . \quad (17)$$

Using eq. (4) indicates that the maximum permissible heat fluxes are

$$q_{hmax} = 7.4/L^{1/3} = 4.45 \text{ W/cm}^2; \quad q_{vmax} = 7.4/L^{1/3} = 5.02 \text{ W/cm}^2. \quad (18)$$

Comparing eqs. (17) and (18), we see that $q_{h,vmax} > q_{h,v}$, which implies that the designed insulation cooling channels are adequate to provide thermal stability to the TMNS conductor configuration operating at 15.6 kA. In fact, since the maximum full recovery current scales as the square root of the maximum transmitted heat flux,

$$\frac{I_{max}}{I} \approx \left(\frac{q_{max}}{q} \right)^{1/2} = \left(\frac{9.47}{7.49} \right)^{1/2} = 1.124 ,$$

which implies that the maximum full recovery current in the TMNS is 17.5 kA or 12.4% higher than the operating current (15.6 kA).

5. STEADY-STATE HEAT TRANSFER, INCLUDING COLD-END RECOVERY

The preceding analysis has ignored the effects of cold ends on the heat-transfer stability. If a given length of conductor becomes normal and experiences a temperature rise while its ends are maintained at the temperature of the coolant bath, the colder ends act together with the channel coolant to enhance the conductor stability via cold-end recovery /3/. The Maddock criterion for cold-end recovery states that the maximum current that will yield recovery is determined by equating the areas of the heat-transfer and heat-generation curves of Fig. 3. This requires that

$$\int_{T_b}^{T_f} \left[G(H_a,I,T) - Q(T) \right] dT = 0. \quad (19)$$

Integrating eqs. (1,3,4,6) between the temperature ranges depicted by eqs. (2,5,6,8) yields an equation for the maximum cold-end recovery current.

Equation (19) requires solving a fourth-degree equation for the current. This is best done by a small computer program into which initial guesses for current are input and the integral in eq. (19) is output. The output of eq. (19) is plotted against the current, and the maximum recovery current is determined by extrapolation through the function zero, as shown in Fig. 7. For the TMNS coil the fully stable recovery current is 17.5 kA, while the cold-end recovery current is 19.85 kA.

6. He-II TRANSIENT STABILITY ANALYSIS

Another important consideration is the effect of transient phenomena on the coil stability. Suppose 10 m of turn X in Fig. 5 goes normal. Since the single turn produces 3.38 W/cm, this corresponds to a total power production of 3380 W, a value greater than the refrigeration capacity at 1.8 K. How long can the conductor remain normal before the He-II in thermal contact with it converts to He-I and film boiling is initiated, or before the electronic quench protection system initiates a

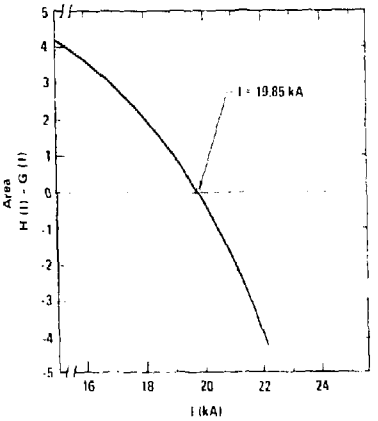

Fig. 7 - TMNS cold end recovery current

magnet discharge? Solving the heat transport and energy balance equations for a single Gorter-Mellink channel,

$$\frac{\partial T}{\partial \tau} = \frac{405.224\ f(T)Q^3}{T_\lambda}, \qquad T(0,\tau) = 1,\ Q(1,0) = Q_0,$$
$$\frac{\partial Q}{\partial \psi} = \frac{C_p(T)T_\lambda}{\Delta E_0}\frac{\partial T}{\partial \tau}, \qquad Q(1,1) = Q(0,\psi) = 0, \tag{20}$$

yields the fractional volume of He-II surrounding a normal turn of conductor that is available to absorb energy from the conductor before the initiation of film boiling. In eq. (20), the dimensionless parameters are

$$T = T/T_\lambda,\ Q = 7.4\ q/L^{1/3},\ \psi = x/L \text{ and } \tau = \frac{7.4\ t}{\Delta E_0 L^{1/3}}, \tag{21}$$

in which ΔE_0 is the enthalpy difference of He-II between 1.8 and 2.17 K. The solution is plotted in Fig. 8 for various values of the ratio $Q = q/q_0$; here q_0 is the maximum steady-state heat flux that a given channel length L can conduct. The corresponding temperature and heat flux profiles down the channel are shown in Figs. 9 and 10 for $Q_0 = 1$. The rather unusual behavior of the heat-flux profile

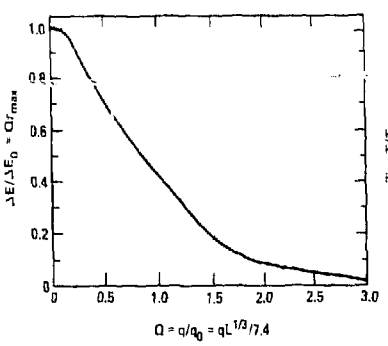

Fig. 8 - Time and available energy absorption before film boiling

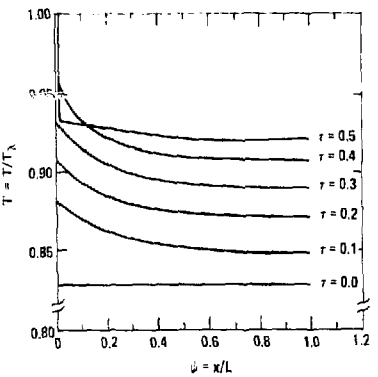

Fig. 9 - Temperature profile at various times. $Q_0 = 1$

at the onset of film boiling has also been calculated for other values of Q_0 and appears to be indicative of a flux-wave instability. Since the results of Section 4 indicate that the case of multiple, interconnecting cooling channels can

be approximately treated as a single Gorter-Mellink channel, with length L equal to the pitch distance, the transient analysis of the TMNS conductor pack is treated using these considerations. Figure 11 contains a plot of the heat-flux profile within a horizontal channel emanating from a normal conductor turn, according to eq. (9). The product of $qL^{1/3}/7.4$ is also plotted versus the zone number N defined by

$$N = L_T/L_{h,v} \ , \tag{22}$$

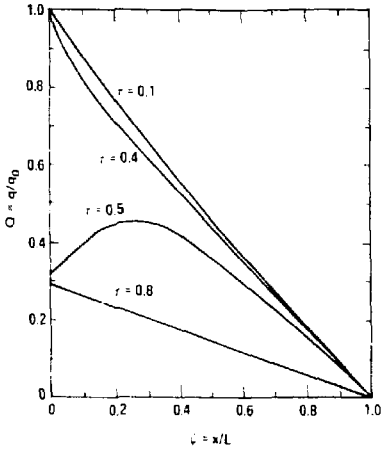

Fig. 10 - Heat flux profile at various times. $Q_0 = 1$

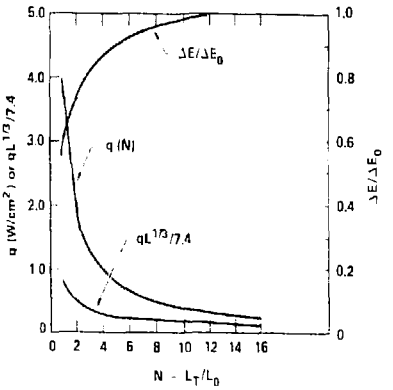

Fig. 11 - Heat flux, and available energy for a TMNS horizontal coolant channel

where L_T is the total distance from conductor X and $L_{h,v}$ are the original horizontal and vertical pitch distances of eq. (16). A plot of the available fluid enthalpy per unit volume which can absorb the conductor energy as a function of distance from the normal turn is also shown in this figure. This plot was generated by comparing the $qL^{1/3}/7.4$ curve with Fig. 10. The time before film boiling occurs can be estimated to be

$$\Delta t = \frac{\Delta E_0 \ < \Delta E/\Delta E_0 > V_{He-II}}{Q} \ , \tag{23}$$

where $< \Delta E/ E_0 >$ is the average value of the curve in Fig. 11, Q is power produced by the normal turn, and V_{He-II} is the total volume of He-II in the coil. Equation (21) can be written as

$$\Delta t = \frac{\Delta E_0 \ < \Delta E/\Delta E_0 > V_0 (2N + 1)^2}{Q} \ , \tag{24}$$

in which V_0 is the volume of He-II surrounding each unit length of conductor and the $(2N + 1)^2$ factor is the number of conductors enclosed in the N_{th} zone. The case when N = 16 corresponds to a 33 x 33 turn conductor pack subcoil. If each subcoil is separately refrigerated at 1.8 K, a normal turn at 15.6 kA is expected to take approximately 87 s before the onset of film boiling at its surface.

7. CONCLUSIONS

The configuration of the conductor-cooling channel for TMNS, shown in Fig. 4, has been shown to be remarkably stable under steady-state and transient operation in subcooled, superfluid He-II. The enhanced behavior over that of He-I coolant can be attributed to two factors: the unique thermophysical properties of He-II and the selection of either "ladder or button" insulation, which produces a network of multiple, branching, coolant-channels.

ACKNOWLEDGMENTS

We would like to extend our sincerest thanks to the many who also contributed to this design study. These include: Dr. S. Van Sciver for his stimulating answers to our questions on He-II heat transfer; Drs. R. Hickman and J. Painter for their assistance with the LSODI differential equation solver; Vergie Zuppan and John Warmouth, who struggled successfully to type and illustrate this paper. This work was performed under the auspices of the U.S. Department of Energy by the Lawrence Livermore National Laboratory under contract number W-7405-ENG-48.

REFERENCES

1. D. N. CORNISH, R. W. HOARD, and R. BALDI: Design of 12-T yin-yang magnets operating in subcooled, superfluid helium. Proc. 9th Symp. Engineering Problems of Fusion Research, Chicago (1981)(to be published).

2. R. W. BALDI and R. E. TATRO: Design scoping study of the 12-T yin-yang magnet system for the tandem mirror next step (TMNS), final report, Lawrence Livermore National Laboratory, UCRL-15405 (1981).

3. B. J. MADDOCK, G. B. JAMES, and W. T. NORRIS: Superconductive composites: heat transfer and steady-state stabilization. Cryogenics (1969), pp. 261-273.

4. S. W. VAN SCIVER: Cryostabilization of large superconducting magnets using pool boiled helium-II. Proc. 6th Symp. on Eng. Problems of Fusion Research, San Diego (1977), pp. 690-694.